



Contents lists available at ScienceDirect



# Catalysis Today

journal homepage: [www.elsevier.com/locate/cattod](http://www.elsevier.com/locate/cattod)

## Efficient dehydration of fructose to 5-hydroxymethylfurfural over sulfonated carbon sphere solid acid catalysts

Jun Zhao<sup>a</sup>, Chunmei Zhou<sup>b</sup>, Chao He<sup>a</sup>, Yihu Dai<sup>a</sup>, Xinli Jia<sup>a</sup>, Yanhui Yang<sup>a,\*</sup>

<sup>a</sup> School of Chemical and Biomedical Engineering, Nanyang Technological University, Singapore 637459, Singapore

<sup>b</sup> School of Materials Science and Engineering, Zhejiang University, Hangzhou 310027, China

### ARTICLE INFO

#### Article history:

Received 1 April 2015

Received in revised form 29 June 2015

Accepted 1 July 2015

Available online xxxx

#### Keywords:

Fructose

Dehydration

HMF

Carbon sphere

### ABSTRACT

A carbon-based solid acid catalyst was prepared via hydrothermal method using glucose as carbon precursors and aqueous solution of H<sub>2</sub>SO<sub>4</sub> as sulfonation agent. The as-synthesized solid acid catalyst was attempted in the catalytic dehydration of fructose to 5-hydroxymethylfurfural (HMF). The effects of acid site density, reaction time, solvents, catalyst amount, temperature and mole ratio of catalyst to substrate were investigated. Under the optimum reaction conditions, the HMF yield of 90% was achieved in dimethylsulfoxide (DMSO) solvent at 160 °C after 1.5 h reaction time duration. The solid acid catalyst can be separated from the reaction mixture after reaction and reused without substantial loss in catalytic activity.

© 2015 Elsevier B.V. All rights reserved.

## 1. Introduction

Biomass is one of promising renewable and sustainable alternatives for energy and chemical production. As an energy source, biomass can either be utilized directly via combustion to produce heat or indirectly after converting to various biofuels. In addition, researchers have recently made considerable progress in transforming biomass to chemicals such as carbohydrates [1–3], and subsequently converting these carbohydrates to valuable intermediates and polymeric materials. Among all the carbohydrates derived from biomass (primarily cellulosic components of biomass), glucose and fructose are economically suitable to be employed as feedstock for the production of downstream value-added chemicals [4–6]. Several chemical processes have been developed to convert glucose and fructose to chemicals, for instance, increasing interest has been devoted to the dehydration of fructose to produce chemical building blocks such as 5-hydroxymethylfurfural (HMF). HMF has been identified as a versatile platform molecule which can be transformed to valuable chemicals such as 2,5-furandicarboxylic acid (FDCA) 2,5-diformylfuran (DFF) and 5-hydroxymethyl-2-furancarboxylic acid (HMFC) that are suitable starting materials for the preparation of polymers [7].

HMF was first separated from the reaction mixture of fructose, sucrose and oxalic acid in 19th century. Nowadays, HMF is mainly produced by the dehydration of monosaccharides. The dehydration process to produce HMF is remarkably complex due to the possible side reactions. For instance, the cross-polymerization of HMF leads to the formation of colored soluble polymers and insoluble brown humins. The dehydration of fructose to HMF can be catalyzed by protonic acid as well as by Lewis acid [8,9]. HCl, H<sub>2</sub>SO<sub>4</sub> and H<sub>3</sub>PO<sub>4</sub> are the most common acids for fructose dehydration to produce HMF. Sulfuric acid afforded a HMF yield as high as 53% in sub-critical water at 250 °C [10,11]. HCl and H<sub>3</sub>PO<sub>4</sub> can also catalyze fructose dehydration in subcritical water, resulting in a HMF yield of 40–50% [12]. Organic acids such as oxalic acid, levulinic acid and *p*-toluenesulfonic acid were attempted as well [13–16]. In addition, Ionic liquids were also designed and applied in the conversion of carbohydrates to HMF [17]. In order to improve the HMF yield, a two-phase reactor was developed in the presence of HCl as the catalyst. Adding dimethylfulfoxide (DMSO) and ploy (1-vinyl-2-pyrrolidinone) (PVP) to the reaction mixture significantly suppressed the undesired side reactions [18], and 80% HMF selectivity at 90% conversion was reported for a 10 wt.% fructose solution. Although the fructose conversion and HMF selectivity can be enhanced by optimizing the reaction parameters, there are still concerns using the above-mentioned liquid acids as catalysts: these conventional homogeneous acid catalysts are difficult to be separated from the reaction mixture, resulting in the product purification and catalyst recycling issues.

\* Corresponding author. Tel.: +65 6316 8940; fax: +65 6794 7553.

E-mail address: [yhyang@ntu.edu.sg](mailto:yhyang@ntu.edu.sg) (Y. Yang).

Solid acid catalysts can overcome the drawbacks of homogeneous catalysts and have been attempted in fructose dehydration. Furthermore, solid acid catalysts are capable of tuning the surface acidity and working at harsh reaction conditions [19]. The fructose conversion of 76% and HMF selectivity of 92% were achieved over de-aluminated H-form mordenite at 165 °C in a solvent consisting of water and MIBK [20,21]. In the presence of vanadylphosphate (VOP), a 40% yield of HMF was obtained in a 6 wt.% aqueous fructose solution [22]. Introducing different trivalent metal cations enhanced the VOP catalytic activity; the yield and selectivity increased to 50% and 87%, respectively over a Fe-containing VOP catalyst. Nb-based catalysts such as  $\text{Nb}_2\text{O}_5$ , niobium phosphate ( $\text{NbPO}_4$ ) and sulfated mesoporous niobium oxide also exhibited high catalytic activity [23–26]. Zr- and Ti-based catalysts with different structures were tried in the dehydration of fructose, HMF yield of 47% was obtained within 4 h at 130 °C over  $\text{SO}_4^{2-}/\text{ZrO}_2-\text{Al}_2\text{O}_3$  with Zr-Al molar ratio of 1:1 [27]. Ion-exchange resin Amberlyst-15 has also been reported as the catalyst for fructose dehydration in aqueous solutions [28].

The carbon-based solid acids, possessing high stability, low cost and abundant strong protonic acid sites on surfaces, have been widely used in hydrolysis, esterification and condensation reactions [29]. In particular, carbon sphere (CS) solid acid catalysts can be prepared by direct sulfonation of CS generated from various carbon precursors such as sugars, polycyclic aromatic compounds, resins, activated carbon, bio-char and lignin [30–32]. In the typical synthesis of CS, glucose, sucrose, fructose or cellulose was heated to 400–600 °C under  $\text{N}_2$  flow to produce black powder. The obtained black powder was then heated in concentrated sulfuric acid or fuming sulfuric acid at 150–200 °C [33–35]. In addition to  $-\text{SO}_3\text{H}$  groups on CS surfaces, there were also  $\text{Ph}-\text{OH}$  and  $-\text{COOH}$  functionalities, resulting in superior performances in liquid-phase acid-catalyzed reactions. Sulfonated CS afforded excellent catalytic performances compared to the sulfonated amorphous glassy carbon, activated carbon and natural graphite [36,37], due to the compact carbon structure of these precursors and the lack of functional groups, particularly acid sites on the surfaces [36,38]. In this work, a modified preparation of carbon-based solid acid under mild conditions was developed. The CS was prepared by hydrothermal carbonization of glucose at 180 °C which was remarkably lower than the temperature in other CS synthetic routes. The resulted CS was sulfonated by sulfuric acid aqueous solutions instead of concentrated  $\text{H}_2\text{SO}_4$  or fuming sulfuric acid. Catalytic results showed that the catalysts afforded high activity for the dehydration of fructose to HMF. Under an optimized condition, fructose was converted into HMF with 90% yield at 160 °C after reaction duration of 1.5 h.

## 2. Experimental

### 2.1. Catalyst preparation

Fructose ( $\geq 99\%$  purity), HMF (99% purity), Glucose ( $\geq 99\%$  purity), sulfuric acid (98% purity) and all the solvents were obtained from Sigma-Aldrich. These commercial chemicals were used as received without further purification. The CS was prepared by hydrothermal carbonization of glucose [39]. In the typical synthesis, 5 g of glucose was dissolved in 30 ml of deionized water to form a clear solution under stirring. The solution was then transferred into a 40 ml capacity teflon-lined autoclave and maintained at 180 °C for 10 h. The resulting solid products were filtered and washed with deionized water and ethyl alcohol, followed by vacuum drying for 4 h at 60 °C to afford CS.

The as-synthesized CS was dispersed in a sulfuric acid solution under stirring. The suspension was placed in a 40 ml teflon-sealed autoclave and maintained at 180 °C for 4 h. The black products were

filtered, washed and then dried following the same procedures in CS preparation. Sulfuric acid solutions with different concentrations were employed in the sulfonation processes. The sulfonated CS solid acid catalysts were labeled as CS-1, CS-2, CS-3 and CS-4 according to the sulfuric acid and water volumetric ratios of 1:5, 1:2, 1:1 and 2:1, respectively. For comparison purposes, sulfonated CS was also prepared in one-step following the procedures as reported by Liu et al. [40]. Equal amounts of glucose dissolved in sulfuric acid solutions of different sulfuric acid and water ratios (1:5, 1:2, 1:1, 2:1); the solutions were placed in teflon-sealed autoclaves and heated at 180 °C for 4 h. The products were labeled as C-1, C-2, C-3 and C-4.

### 2.2. Catalysts characterization

Fourier transform infrared (FTIR) spectra were obtained on Digilab FTS 3100 FTIR with a  $4\text{ cm}^{-1}$  resolution in the range of 400–4000  $\text{cm}^{-1}$  using a standard KBr disk technique. Raman tests were carried out on a Renishaw 1000 Raman spectrometer equipped with a 514 nm excitation from HeNe laser, of which the detection depth is about 150 nm. The BET surface areas were measured on Autosorb-6B (Quantachrome instruments) using the liquid nitrogen adsorption method. Powder X-ray diffraction (XRD) patterns were recorded on a Bruker Advance 8 X-ray diffractometer using a Ni filtered  $\text{Cu K}\alpha$  radiation ( $\lambda = 0.154\text{ nm}$ ), operated at 40 kV and 40 mA. XRD data were collected between 10 and 90° ( $\theta$ ) with a resolution of 0.02° ( $\theta$ ). The morphology and structure of the spheres were investigated using a field emission scanning electron microscope (FESEM, JOEL JSM 6701F). Temperature-programmed desorption (TPD) was performed on a Micromeritics AutoChem II 2920 instrument. Typically, the pretreatment of the sample was conducted in a quartz reactor by high-purity Ar at 200 °C for 2 h. Then after the temperature cooled down to 100 °C, it was set to rise to 1020 °C at a rate of 5 °C/min. A mass spectrometer (ThermoStar GSD 301 T2) was used to detect the desorbed CO and  $\text{CO}_2$ . In addition, 1H-NMR spectra were measured to analysis the separated product on a Bruker Avance II 300 MHz spectrometer with  $\text{CDCl}_3$  as the solvent. The element composition of the catalyst was estimated by Vario EL III CHNS Elemental Analyser.

The total number of acid sites on the catalyst surfaces were determined by a well-established acid-base back neutralization titration method [41]. The CS catalyst (30 mg) was suspended in a sodium hydroxide aqueous solution (0.1 M, 20 ml). The mixture was stirred using a magnetic stirrer for 4 h, followed by ultrasonication for 1 h at room temperature. The concentration of the  $\text{OH}^-$  ions in the supernatant solution was calibrated by oxalic acid standard solution. The content of  $-\text{SO}_3\text{H}$  groups on the surfaces of the CSs were determined by neutralization titration with sodium hydroxide. A sodium chloride aqueous solution (0.2 M, 20 ml) was added to the catalyst (30 mg). The mixture was stirred using a magnetic stirrer for 4 h, followed by ultrasonication for 1 h at room temperature. The supernatant solution was titrated using a sodium hydroxide (0.01 M) solution.

### 2.3. Catalytic reactions

The catalytic reaction was performed in a 25 ml capacity flask equipped with a condenser. In a typical catalytic run, a DMSO solution of fructose (0.5 g of fructose in 10 ml of DMSO) was added into the flask along with 100 mg of CS solid acid catalysts. The reaction mixture was heated to the reaction temperature in oil bath with a thermostat and an electronically controlled magnetic stirrer. The reaction samples were removed periodically and analyzed. The reaction products were diluted in water and filtered through a syringe filter (VWR, 0.22  $\mu\text{m}$  PTFE) prior to analysis by liquid chromatography (HPLC, Agilent 1100 series, Bio-Rad Aminex HPX-87H,

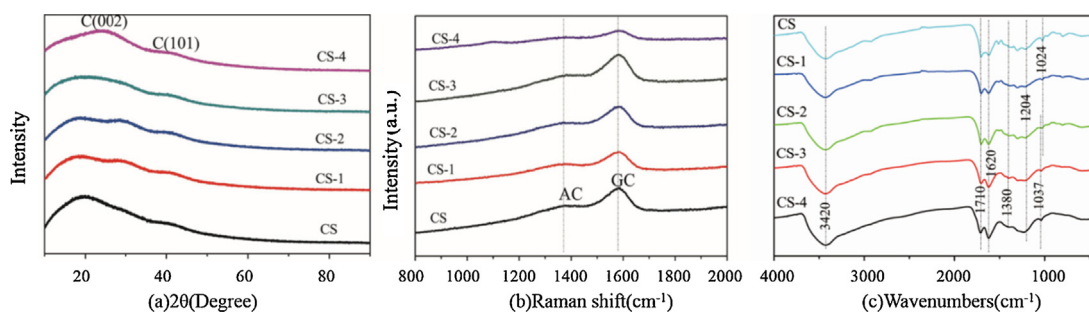


**Fig. 1.** (a) XRD patterns of CS, CS-1, CS-2, CS-3 and CS-4, (b) Raman spectra of CS, CS-1, CS-2, CS-3 and CS-4, (c) FTIR spectra of CS, CS-1, CS-2, CS-3 and CS-4.

300 mm × 7.8 mm pre-packed column). Sulfuric acid (5 mM H<sub>2</sub>SO<sub>4</sub>) was employed as the mobile phase at a flowing rate of 0.6 ml/min at 60 °C. Reactant conversion (mol%), HMF yield (mol%) and product selectivity (%) were defined as follows:

$$\text{Conversion (mol\%)} = \frac{\text{moles of fructose reacted}}{\text{moles of initial fructose}} \times 100\%$$

$$\text{Yield (mol\%)} = \frac{\text{moles of HMF produced}}{\text{moles of initial fructose}} \times 100\%$$

$$\text{Selectivity (\%)} = \frac{\text{moles of HMF produced}}{\text{moles of fructose reacted}} \times 100\%$$

### 3. Results and discussion

#### 3.1. Characterization of CS catalysts

The XRD patterns of synthesized CS solid acids are shown in Fig. 1(a). The weak diffraction peaks at 2θ angles of 10–30° and 35–50° are attributed to the (0 0 2) and (1 0 1) planes of amorphous carbon, respectively, indicating the carbonization of the glucose

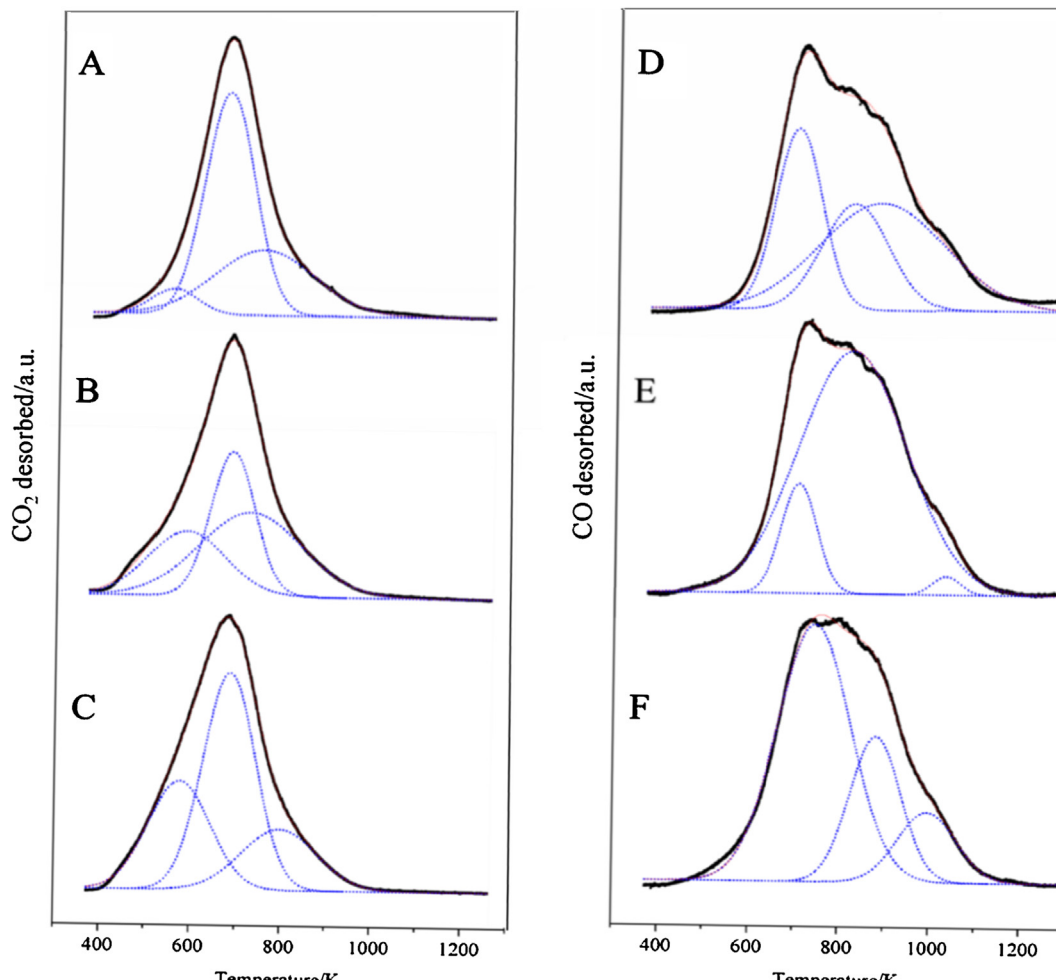


**Fig. 2.** TPD profiles for carbon spheres. A-C CO<sub>2</sub> desorption profiles, D-F CO desorption profiles. A and D are carbon spheres before sulfonation, B and E are carbon spheres after sulfonation, C and F are sulfonated carbon spheres recycled after dehydration reaction.

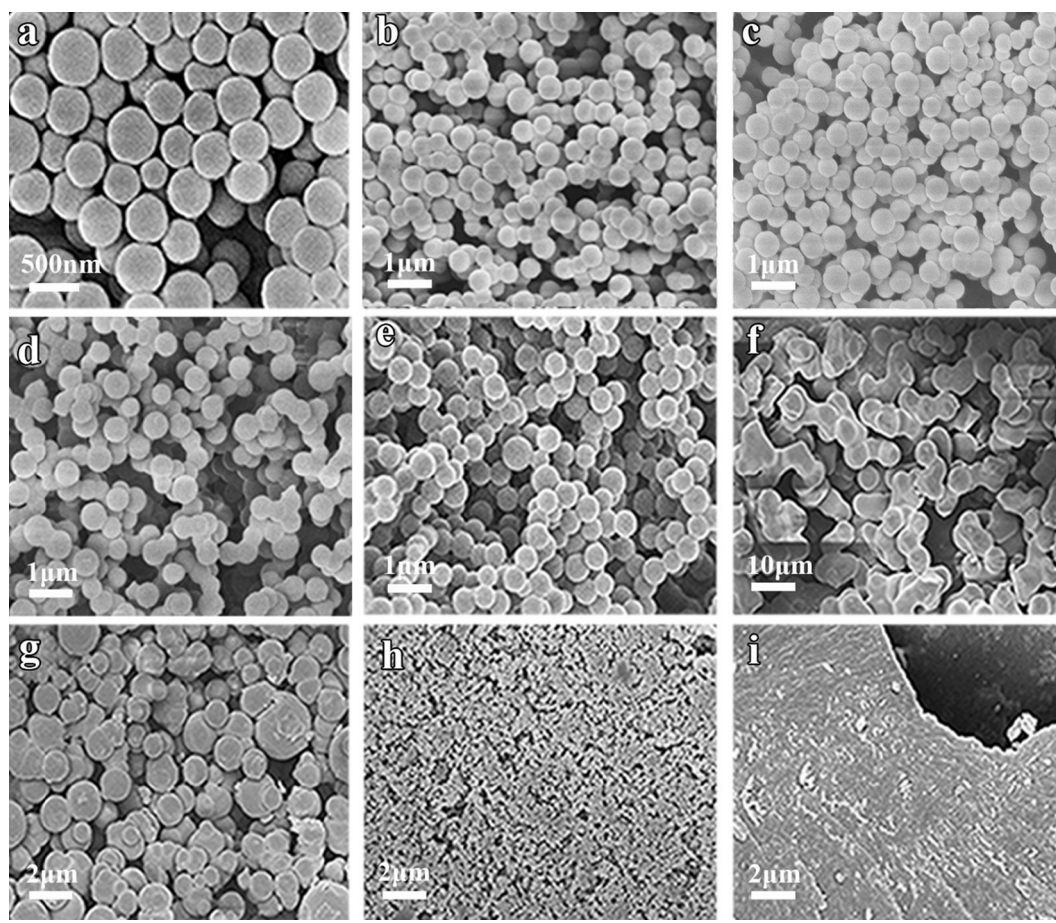


**Fig. 3.** FESEM images of: (a) CS, (b) CS-1, (c) CS-2, (d) CS-3, (e) CS-4, (f) C-1, (g) C-2, (h) C-3, (i) C-4.

precursors [36,42]. All the samples display two broad signals D-band ( $1390\text{ cm}^{-1}$ , A<sub>1g</sub> D breathing mode) and G-band ( $1590\text{ cm}^{-1}$ , E<sub>2g</sub> G mode) in the Raman spectra as shown in Fig. 1(b). The peak intensity ratios of D- to G-band of these CS materials are nearly the same, implying the similar average graphene sizes of these CSs [43]. The FTIR spectra of these CS samples are shown in Fig. 1(3). The absorption band at  $1037\text{ cm}^{-1}$  is assigned to  $-\text{SO}_3\text{H}$  groups, showing that the  $-\text{SO}_3\text{H}$  groups are successfully linked onto the CS surfaces. The bands attributed to  $-\text{OH}$  group at  $3420\text{ cm}^{-1}$ , C=O group at  $1720\text{ cm}^{-1}$  and C–O group at  $1203\text{ cm}^{-1}$  suggest the presence of  $-\text{COOH}$  groups. The peaks at  $1620$  and  $1380\text{ cm}^{-1}$  are attributed to C=C groups.

The oxygen-containing functional groups on the surfaces are further studied by TPD and the relative concentrations of various functional groups including carboxyl, anhydride, ester, phenol and carbonyl/quinone are shown in Fig. 2, and summarized in Table 1. The sequence of temperatures for decomposition of the oxygen-containing groups to produce CO<sub>2</sub> and CO upon heating is carboxyl < anhydride < ester and anhydride < phenol < carbonyl/quinone. The relative concentrations of different functional groups are estimated by means of overlapping peak deconvolution. As seen in Table 1, for the CS after sulfonation, the relative concentrations of carboxyl, ester and phenol groups increase while those of anhydride and carbonyl/quinone decrease. After reaction, the concentrations of carbonyl/quinone and carboxyl groups increase due to the hydrolysis of ester groups and the loss of phenol groups. However, the catalytic reaction results and recycle experiments suggest that the catalytic activities remain the same although the type and quantity of these functional groups change.

SEM images shown in Fig. 3 reveal that the CSs prepared by the two-step method possess narrow distributed granular diameters of approximately 400–500 nm regardless the concentration of sulfuric acid solutions. On the other hand, those CSs prepared by the one-step method show irregular shapes with wide size distributions. Furthermore, particle agglomeration occurs significantly on the CSs prepared by the one-step method. The products C-1, C-2, C-3 and C-4 prepared by the one-step hydrothermal method show different morphological features depending on the concentration of the sulfonating solution. The diameter of C-1 sphere is in the range of 5–8  $\mu\text{m}$  while it decreases to 1–4  $\mu\text{m}$  as the concentration of the sulfonating solution is doubled (C-2). C-3 and C-4 are primarily formed by the aggregation of fine particles and the particle sizes of C-4 are remarkably smaller than those of C-3.

**Table 1**

Relative concentration of functional groups over the CS catalysts<sup>a</sup>.

Functional groups	CS	CS acid	CS acid <sup>b</sup>
CO <sub>2</sub> desorption peak			
Carboxyl	17	73	100
Anhydride	97	56	100
Ester	77	100	53
CO desorption peak			
Anhydride	45	18	100
Phenol	32	100	34
Carbonyl/quinone	100	3	30

<sup>a</sup> Estimated from the desorbed CO and CO<sub>2</sub> peaks in TPD spectra, the concentration of the strongest peak for each functional groups among the three samples has been normalized to 100.

<sup>b</sup> The catalyst sample was collected after reaction.

**Table 2**

The physicochemical properties of the catalysts.

	Surface area ( $\text{m}^2/\text{g}$ )	$\text{SO}_3\text{H}$ amount (mmol/g)	Acid density (mmol/g)
CS-1	26.70	0.09	8.53
CS-2	40.17	0.17	7.90
CS-3	153.75	0.32	7.89
CS-4	357.43	0.71	7.79

The strength and density of acid sites of carbon-based solid acid is a vital factor closely related to the catalytic activity [27]. The sulfonated CSs have both strong and weak acid sites on the surfaces. As shown in Table 2, the total acid density on the surface is almost the same for CS-1, CS-2, CS-3 and CS-4 regardless the concentration of sulfonating solution, while the amount of  $-\text{SO}_3\text{H}$  increases from CS-1 to CS-4 with increasing the concentration of the sulfuric acid solutions. The BET surface areas of CSs also show correlation with the concentrations of the sulfonating solutions as shown in Table 2; the areas increase from 26.7 to 357.4  $\text{m}^2/\text{g}$  as the sulfuric acid concentrations increase. The BET surface areas of the CSs synthesized by one-step hydrothermal carbonization are remarkably smaller compared to those of prepared by the two-step method [40].

### 3.2. Catalytic performance of catalysts

#### 3.2.1. Effect of solvent

Solvents usually play a significant role in liquid phase catalytic reactions and in this study the solvent effects on the dehydration of fructose to HMF are shown in Fig. 4. Among the solvents tested, DMSO is the best for fructose dehydration to HMF, showing superior catalytic performances. Amarasekara et al. [44] suggested that DMSO acted as the catalyst in the process of fructose dehydration. To verify the solvent effect of DMSO, a blank experiment in the absence of catalyst is conducted in DMSO. Fructose conversion of 56.4% and HMF selectivity of 22.4% can be achieved in 0.5 h at 140 °C. Furthermore, by using DMSO and DMF mixture (volume ratio of 1:4) as solvent, 93.1% of fructose conversion and 52.2% of HMF yield are obtained in the presence of CS-2 catalyst, while these two values are only 29.3% and less than 2%, respectively without catalysts. Reactions in toluene and ethylene glycol show extremely high fructose conversion (99.1% and 82.7%, respectively). Nonetheless, the HMF selectivity is less than 2% after 2 h reaction duration, implying the presence of significant side reactions. Caratzoulas and Vlachos [45] studied the solvent effects using hybrid Quantum Mechanics/Molecular Mechanics Molecular Dynamics simulations and found that the activation energy for the hydride transfer in

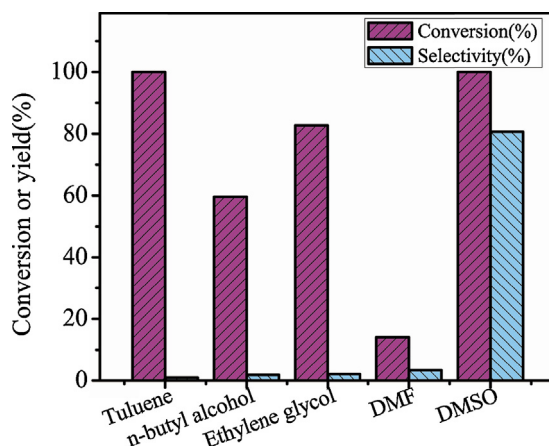


Fig. 4. Dehydration of fructose in different solvents. Reaction conditions: fructose (500 mg), catalyst (100 mg), solvent (10 ml), 140 °C for 2 h.

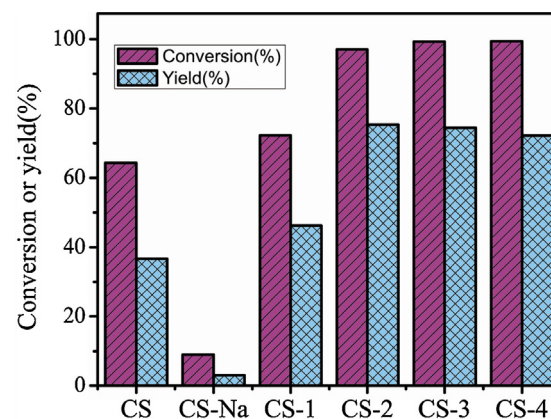


Fig. 5. Dehydration of fructose by different catalysts. Reaction conditions: fructose (500 mg), catalyst (100 mg), DMSO (10 ml), 140 °C for 0.5 h.

fructose dehydration was closely related with the polar solvent environment. According to the further study by Vlachos et al. [51], DMSO solvents arranged themselves in the immediate vicinity of hydrogen atoms of the hydroxyl groups in fructose, helped prevent fructose from forming reversion and polymerization products. On the other hand, DMSO molecules around C1 atom of HMF hindered the rehydration of HMF and humins formation.

#### 3.2.2. Effect of the acid site density over the catalyst

CS catalysts with different amounts of  $-\text{SO}_3\text{H}$  groups on surfaces are attempted in the dehydration of fructose to HMF, and the results are shown in Fig. 5. Amberlyst-15 and SBA- $\text{SO}_3\text{H}$  have been reported as solid acid catalysts to catalyze fructose dehydration to HMF [28], and sulfonic acid groups were suggested as the active sites in this particular reaction. Nonetheless, it can be seen from Fig. 5, CS catalyst in the absence of any sulfonic acid groups shows a reasonably good catalytic performance with fructose conversion of 64.3% and HMF yield of 36.7% in 0.5 h reaction duration, implying that other surface acid groups such as  $-\text{COOH}$  also show catalytic activity in this reaction [12]. Introducing sulfonic acid groups significantly improves the catalytic activity. The fructose conversion and HMF yield are above 97% and 75%, respectively over CS-2 and CS-3. CS-2 affords the highest HMF selectivity of 77%. Under the same reaction conditions, a fructose conversion of only 9% and HMF yield of 3% are obtained when the reaction is catalyzed by CS-Na which is prepared by ion-exchange  $\text{H}^+$  by  $\text{Na}^+$  over CS-2, indicating the important role of protonic acid in the dehydration of fructose to HMF. Generally, the more the sulfonic groups on CS catalyst surfaces, the higher the conversion and yield of catalytic performances, as shown in Fig. 5 over catalysts from CS-1 to CS-3. As for CS-4, the yield of HMF decreases slightly because HMF proceeds further decomposition due to the remarkably high sulfonic acid site density over CS-4 surfaces, the amounts of sulfonic acid groups of CS-4 is two times higher than that of CS-3 [46]. Furthermore, the conversion of sucrose to HMF is also conducted using the CS solid acid as catalyst and 91.1% HMF yield can be reached in 6 h in DMSO at 140 °C, indicating the superior catalytic activity of CS solid acid catalysts.

#### 3.2.3. Catalytic role of the $\text{S=O}$ group

DMSO acted as both solvent and catalyst in the dehydration of fructose to HMF and  $\text{S=O}$  group in DMSO was proposed to be the catalytic active site [44]. In this study, different type and quantity of salts in which there are  $\text{S=O}$  structures are added into the reaction system as the control experiments to further verify the role of sulfonic groups on the catalytic reactions (Table 3). When adding  $\text{H}_2\text{SO}_4$  as the catalyst, fructose conversion of 85.34% and HMF yield

**Table 3**

The catalytic reaction results for the dehydration of fructose to HMF with different acid catalysts and salts.

Entry	Catalyst	Salt	T (°C)	Time (min)	Fructose conv. (%)	HMF sel. (%)	HMF yield (%)
1	H <sub>2</sub> SO <sub>4</sub>	–	125	30	85.34	79.05	67.46
2	H <sub>2</sub> SO <sub>4</sub>	Na <sub>2</sub> SO <sub>4</sub>	125	30	76.91	68.50	52.68
3 <sup>a</sup>	H <sub>2</sub> SO <sub>4</sub>	Na <sub>2</sub> SO <sub>4</sub>	125	30	65.05	63.98	41.62
4	CS-2	–	125	30	86.30	71.94	62.08
5	CS-2	Na <sub>2</sub> SO <sub>4</sub>	125	30	63.63	67.36	42.86
6	CS-2	C <sub>8</sub> H <sub>7</sub> SO <sub>3</sub> Na	125	30	93.09	70.03	65.19
7	–	Na <sub>2</sub> SO <sub>4</sub>	125	30	3.04	–	–
8	–	C <sub>8</sub> H <sub>7</sub> SO <sub>3</sub> Na	125	30	34.59	35.36	12.23

<sup>a</sup> The amount of Na<sub>2</sub>SO<sub>4</sub> of entry is two times of entry 2.

of 67.46% are achieved (**Table 3**, Entry 1), while adding Na<sub>2</sub>SO<sub>4</sub> results in the decrease both in fructose conversion and HMF selectivity (**Table 3**, Entry 2), and the further decrease occurs when more Na<sub>2</sub>SO<sub>4</sub> is added (**Table 3**, Entry 3). Similar results are observed when using CS as the catalyst instead of H<sub>2</sub>SO<sub>4</sub>. Fructose conversion decreases from 86.3% to 63.63% and the yield of HMF decreases from 62.08% to 42.86% due to the addition of Na<sub>2</sub>SO<sub>4</sub> (**Table 3**, Entry 4, 5). These results suggest that the S=O structure in  $\text{SO}_4^{2-}$  shows negative effect in converting fructose to HMF, affording the production of humins and levulinic acid. However, adding styrene-4-sulfonic acid sodium salt in the reaction mixture enhances the efficiency (**Table 3**, Entry 6). Control experiments (**Table 3**, Entry 7, 8) show that styrene-4-sulfonic acid sodium has more remarkable catalytic effects than Na<sub>2</sub>SO<sub>4</sub>. Therefore, the S=O structure in  $\text{SO}_3^-$  acts as a co-catalyst in the reaction, and the  $\text{SO}_3^-$  group on the surface of the CS acid promotes the reaction to certain extent.

### 3.2.4. Effect of catalyst/substrate ratio

A series of experiments are conducted at different catalyst/substrate ratios (5%, 10%, 20%, 30%, and 40%) at 140 °C in DMSO using CS-2 as a representative catalyst, and the results are presented in **Fig. 6**. Gradually, the conversion increases from 86.5% to 100% as the CS-2/fructose ratio increases from 5% to 40%, while the HMF yield first increases from 60.7% (catalyst/substrate ratios 5%) to 75.4% (catalyst/substrate ratios 20%), followed by slightly decreasing to 70.8% (catalyst/substrate ratios 40%). This decrease in yield is attributed to the increasing amounts of catalyst which causes abundant acid sites in the reaction environment, and the side-reactions such as converting HMF to levulinic acid occurs under such conditions [46].

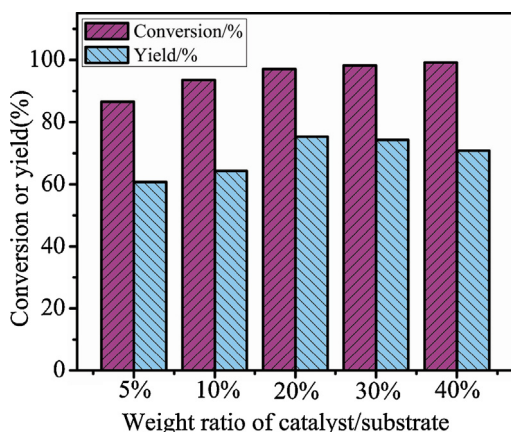


**Fig. 6.** The influence of ratio of catalyst/substrate on the conversion and HMF selectivity. Reaction conditions: fructose (500 mg), catalyst (following the ratio), DMSO (10 ml), 140 °C for 0.5 h.

### 3.2.5. Effect of temperature

The reaction is carried out at different temperatures from 100 to 160 °C and the results are summarized in **Fig. 7**. The conversion of fructose is only 12.8% at 100 °C after 0.5 h. The conversion reaches 100% within the same reaction time duration at 160 °C. The selectivity of HMF also increases from 40.5 to 76.3% as the temperature increases from 100 to 160 °C. When the temperature is higher than 140 °C, the reaction finishes (100% conversion) in 1.5 h. Longer reaction time leads to the slight decrease in HMF yield because HMF is unstable under high temperatures [47].

### 3.2.6. Effect of reaction time

The effect of reaction time duration on the reaction is also investigated and the results are shown in **Fig. 7**. The fructose conversion, HMF selectivity and yield keep increasing along with the reaction time as far as the reaction temperature is below 140 °C though there is a little decrease in the growth rate. When conducting the reaction at the temperature higher than 140 °C, the conversion of fructose quickly reaches almost 100%, indicating the superior catalytic activity, while the selectivity of HMF first increases then decreases, e.g., **Fig. 7(d)** shows the reaction conducted at 160 °C, the HMF selectivity increases from 76.3% (0.5 h) to 90.1% (1.5 h) then decreases to 75.6% (2 h). This decrease in selectivity suggests that the long reaction time leads to the further condensation of HMF into byproducts especially at high reaction temperature [18,48].

### 3.2.7. The adsorption properties test

The adsorption of fructose and HMF by CS is studied in DMSO solution at room temperature. A certain amount of CS is added into 5 ml DMSO solution containing 480 mg of fructose or 100 mg of HMF. The suspension is filtered and analyzed by HPLC after stirring for 6 h under room temperature. As shown in **Table 4**, the catalyst adsorbs fructose in the solution but hardly adsorbs HMF. The adsorption amount of fructose is remarkably higher compared with Amberlyst-15 [49]. The strong adsorption of reactant and quick desorption of product play an important role in affording the high catalytic activity and good selectivity toward desired product.

### 3.2.8. Reusability of the catalyst

The results of stability and reusability of the catalyst are shown in **Fig. 8**. After each reaction run, the catalyst is separated from the reaction mixture and washed with hot water and ethanol, then dried under vacuum at 80 °C for 4 h. There is a slight decrease in both fructose conversion and HMF selectivity after the first run. The conversion and selectivity remain constant during the following cycles. Fructose conversion of 96.2% and HMF selectivity of 73.9% can be maintained even after the 5th run, indicating a good recyclability of the catalyst. A leaching test was conducted to further study the stability of  $\text{SO}_3^-$  groups. 100 mg of catalyst was dissolved in 10 ml DMSO, heated at 140 °C and stirred for 2 h. Then the solution was filtered and the filtrate was used to conduct the dehydration experiment. As shown in **Fig. S1**, the fructose conversion and HMF yield are similar to that of a blank experiment, indicating the high

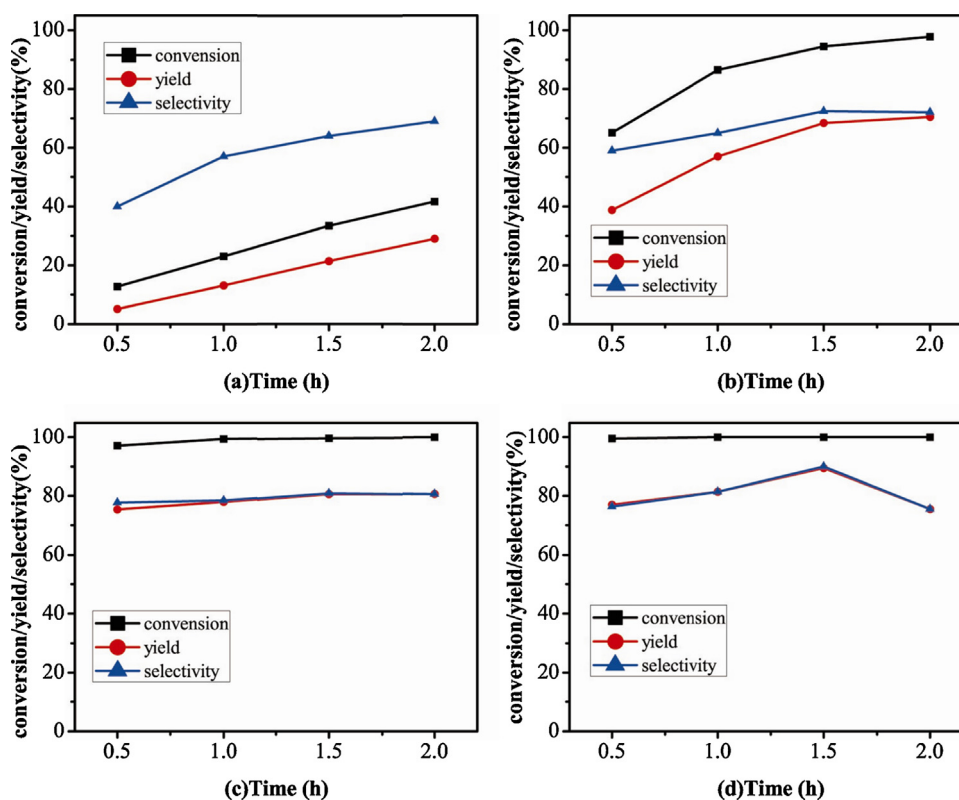


**Fig. 7.** Influence of reaction time and temperature on the dehydration of fructose to HMF. Reaction conditions: fructose (500 mg), catalyst (100 mg), DMSO (10 ml), (a) 100 °C, (b) 120 °C, (c) 140 °C, (d) 160 °C.

**Table 4**  
The adsorption properties of fructose or HMF by CS.

Catalyst	Adsorption of HMF			Adsorption of fructose		
	Initial concentration (mg)	Equilibrium concentration (mg)	R	Initial concentration (mg)	Equilibrium concentration (mg)	R
Blank	100	100	–	480	446	–
CS	100	100	0	480	308	327

R represents the adsorption quantity of HMF or fructose per gram of catalyst (mg/g).

stability of  $\text{SO}_3\text{H}$ . It was confirmed by element analysis that the S content in the catalyst was almost constant (Table S1). In addition, the morphology of the catalyst did not substantially changed after the reaction (Fig. S2).

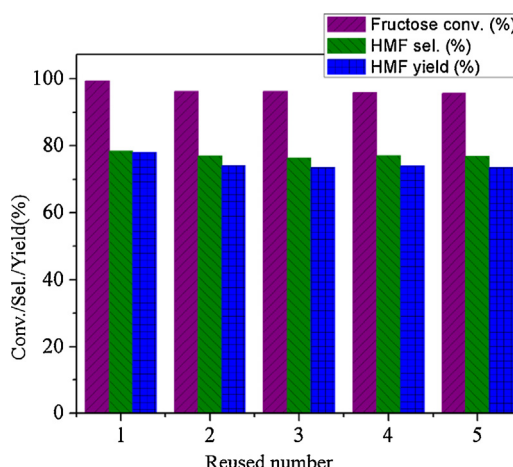


**Fig. 8.** Fructose conversions and selectivity towards HMF in the recycling runs. Reaction conditions: fructose (500 mg), catalyst (100 mg), DMSO (10 ml), 140 °C, 1 h.

### 3.2.9. Discussion

The dehydration of fructose to HMF is an acid-catalyzed reaction consisting of several steps such as protonation, dehydration and deprotonation. Sulfonated CS catalyst, as a strong protonic acid, is suitable for the conversion of fructose to HMF and usually a higher acid density affords better catalytic performances. Carbon-based solid acids are commonly prepared by the sulfonation of different carbon precursors. Konwar et al. [50] studied the influence of different carbon precursors in the preparation of carbon-based solid acid and found that highly carbonized materials were difficult to be sulfonated. In this study, the CSs prepared from the aromatization and carbonization of glucose under hydrothermal conditions were incomplete carbonation materials [39], and they were easy to be sulfonated with high density  $\text{SO}_3\text{H}$  groups on surfaces, showing superior catalytic performances. Different from the CSs prepared by one-step method, the size and morphology of CSs prepared by the two-step method did not change with the concentrations of sulfuric acid solutions, indicating its stable structure and possibility of tuning the acid density on surfaces without changing the carbon-based support. Furthermore, the large surface areas due to the low degree of agglomeration afforded surfaces for  $\text{SO}_3\text{H}$  groups grafting in the sulfonation step and enhanced the contact between fructose and  $\text{SO}_3\text{H}$  groups in the reaction, which contributed to the high catalytic efficiency. Moreover, the

strong fructose adsorption and quick HMF desorption capabilities of the CS contributed to the catalytic performances.

In addition to the catalyst, selection of solvent also played an important role in fructose dehydration. There may have two reaction pathways in the dehydration of fructose to HMF in the presence of DMSO solvent. Amarasekara et al. [44] demonstrated that DMSO catalyzed the dehydration of fructose to HMF due to the S=O bond in DMSO that acted as the catalyst. Similarly, the S=O structure in the  $-\text{SO}_3\text{H}$  groups on CS solid acid surfaces can play the similar role. Therefore, in the presence of CS solid acid, both protonic acid-catalysis (Bronsted acid catalysis) and S=O-catalysis synergistically worked in the reaction system. In addition, the DMSO solvent prevented fructose from side reactions such as the rehydration of HMF to levulinic acid, formic acid and humins because the cleavage of C1 carbon in HMF led to the hydration of HMF to levulinic acid and formic acid. DMSO preferred stay in coordination with the hydroxyl group and C1 carbon in HMF, which effectively provided a shielding effect to the HMF molecule [51].

#### 4. Conclusions

In summary, a sulfonated CS solid acid catalyst bearing  $-\text{SO}_3\text{H}$ ,  $-\text{OH}$  and  $-\text{COOH}$  groups was synthesized by a two-step hydrothermal method. Aqueous sulfuric acid solution replaced the concentrated or fumed sulfuric in the sulfonation step. The acid density and BET surface area of these CS solid acid catalysts increased with the concentrations of the sulfonation solution. The catalyst showed good performances in the dehydration of fructose to HMF under mild conditions, e.g., 100% fructose conversion can be obtained in 0.5 h and HMF yield can reach 90% in 1.5 h at 160 °C. High acid density and reaction temperature accelerated the reaction and improved the selectivity. Nonetheless, excessive amounts of acid sites and high temperature resulted in slight decrease in HMF selectivity due to the further condensation of HMF into byproducts. Besides, high purity HMF can be obtained through extraction by tetrahydrofuran [9] (Fig. S3) and there was no significant loss in activity after five catalytic cycles, indicating the high stability and reusability of the catalyst.

#### Acknowledgements

This project is funded by the National Research Foundation (NRF), Prime Minister's Office, Singapore under its Campus for Research Excellence and Technological Enterprise (CREATE) program. Authors also thank to the financial support from AcRF Tier 1 grant (RG129/14), Ministry of Education, Singapore.

#### Appendix A. Supplementary data

Supplementary data associated with this article can be found, in the online version, at <http://dx.doi.org/10.1016/j.cattod.2015.07.005>

#### References

- [1] B. Hahn-Hagerdal, M. Galbe, M.F. Gorwa-Grauslund, G. Liden, G. Zacchi, *Trends Biotechnol.* 24 (12) (2006) 549–556.
- [2] C.H. Christensen, J. Rass-Hansen, C.C. Marsden, E. Taarning, K. Egeblad, *ChemSusChem* 1 (4) (2008) 283–289.
- [3] J.B. Binder, R.T. Raines, *J. Am. Chem. Soc.* 131 (5) (2009) 1979–1985.
- [4] B.F.M. Kuster, *Starch—Stärke* 42 (8) (1990) 314–321.
- [5] A. Corma, S. Iborra, A. Velty, *Chem. Rev.* 107 (6) (2007) 2411–2502.
- [6] J.N. Chheda, G.W. Huber, J.A. Dumesic, *Angew. Chem. Int. Ed.* 46 (38) (2007) 7164–7183.
- [7] A. Gandini, M.N. Belgacem, *J. Polym. Environ.* 10 (3) (2002) 105–114.
- [8] S. Hu, Z. Zhang, Y. Zhou, J. Song, H. Fan, B. Han, *Green Chem.* 11 (6) (2009) 873–877.
- [9] J.Y.G. Chan, Y. Zhang, *ChemSusChem* 2 (8) (2009) 731–734.
- [10] J.N. Chheda, Y. Roman-Leshkov, J.A. Dumesic, *Green Chem.* 9 (4) (2007) 342–350.
- [11] T.S. Hansen, J.M. Woodley, A. Riisager, *Carbohydr. Res.* 344 (18) (2009) 2568–2572.
- [12] F. Salak Asghari, H. Yoshida, *Ind. Eng. Chem. Res.* 45 (7) (2006) 2163–2173.
- [13] D.W. Brown, A.J. Floyd, R.G. Kinsman, Roshanhyphen, Y. Ali, *J. Chem. Technol. Biotechnol.* 32 (7–12) (1982) 920–924.
- [14] C. Moreau, A. Finiels, L. Vanoye, *J. Mol. Catal. A: Chem.* 253 (1–2) (2006) 165–169.
- [15] B.F.M. Kuster, J. Laurens, *Starch—Stärke* 29 (5) (1977) 172–176.
- [16] J.-D. Chen, B.F.M. Kuster, K. Van Der Wiele, *Biomass Bioenergy* 1 (4) (1991) 217–223.
- [17] S. Siankevich, Z. Fei, R. Scopelliti, G. Laurenczy, S. Katsyuba, N. Yan, et al., *ChemSusChem* 7 (6) (2014) 1647–1654.
- [18] Y. Roman-Leshkov, J.N. Chheda, J.A. Dumesic, *Science* 312 (5782) (2006) 1933–1937.
- [19] X. Tong, Y. Ma, Y. Li, *Appl. Catal., A: Gen.* 385 (1–2) (2010) 1–13.
- [20] C. Moreau, R. Durand, C. Pourcheron, S. Razigade, *Ind. Crops Prod.* 3 (1–2) (1994) 85–90.
- [21] C. Moreau, R. Durand, S. Razigade, J. Duhamet, P. Faugeras, P. Rivalier, et al., *Appl. Catal., A: Gen.* 145 (1–2) (1996) 211–224.
- [22] C. Carlini, P. Patrono, A.M.R. Galletti, G. Sbrana, *Appl. Catal., A: Gen.* 275 (1–2) (2004) 111–118.
- [23] C. Carlini, M. Giuttari, A. Maria Raspolli Galletti, G. Sbrana, T. Armaroli, G. Busca, *Appl. Catal., A: Gen.* 183 (2) (1999) 295–302.
- [24] T. Armaroli, G. Busca, C. Carlini, M. Giuttari, A.M. Raspolli Galletti, G. Sbrana, *J. Mol. Catal. A: Chem.* 151 (1–2) (2000) 233–243.
- [25] P. Carniti, A. Gervasi, S. Biella, A. Auroux, *Catal. Today* 118 (3–4) (2006) 373–378.
- [26] E.L.S. Ngue, Y. Gao, X. Chen, T.M. Lee, Z. Hu, D. Zhao, et al., *Ind. Eng. Chem. Res.* 53 (37) (2014) 14225–14233.
- [27] H. Yan, Y. Yang, D. Tong, X. Xiang, C. Hu, *Catal. Commun.* 10 (11) (2009) 1558–1563.
- [28] K.-i. Shimizu, R. Uozumi, A. Satsuma, *Catal. Commun.* 10 (14) (2009) 1849–1853.
- [29] M.G. Mazzotta, D. Gupta, B. Saha, A.K. Patra, A. Bhaumik, M.M. Abu-Omar, *ChemSusChem* 7 (8) (2014) 2342–2350.
- [30] X. Qi, N. Liu, Y. Lian, *RSC Adv.* 5 (23) (2015) 17526–17531.
- [31] L. Yan, N. Liu, Y. Wang, H. Machida, X. Qi, *Bioresour. Technol.* 173 (0) (2014) 462–466.
- [32] F. Guo, Z. Fang, T.-J. Zhou, *Bioresour. Technol.* 112 (0) (2012) 313–318.
- [33] J.T. Yu, A.M. Dehkhhoda, N. Ellis, *Energy Fuels* 25 (1) (2010) 337–344.
- [34] X. Mo, E. Lotero, C. Lu, Y. Liu, J. Goodwin, *Catal. Lett.* 123 (1–2) (2008) 1–6.
- [35] L. Hu, G. Zhao, X. Tang, Z. Wu, J. Xu, L. Lin, et al., *Bioresour. Technol.* 148 (0) (2013) 501–507.
- [36] M. Okamura, A. Takagaki, M. Toda, J.N. Kondo, K. Domen, T. Tatsumi, et al., *Chem. Mater.* 18 (13) (2006) 3039–3045.
- [37] X. Qi, H. Guo, L. Li, R.L. Smith, *ChemSusChem* 5 (11) (2012) 2215–2220.
- [38] M.-H. Zong, Z.-Q. Duan, W.-Y. Lou, T.J. Smith, H. Wu, *Green Chem.* 9 (5) (2007) 434–437.
- [39] X. Sun, Y. Li, *Angew. Chem. Int. Ed.* 43 (5) (2004) 597–601.
- [40] Y. Liu, Y. Fang, X. Lu, Z. Wei, X. Li, *Chem. Eng. J.* 229 (0) (2013) 105–110.
- [41] T. Liu, Z. Li, W. Li, C. Shi, Y. Wang, *Bioresour. Technol.* 133 (0) (2013) 618–621.
- [42] M. Hara, T. Yoshida, A. Takagaki, T. Takata, J.N. Kondo, S. Hayashi, et al., *Angew. Chem. Int. Ed.* 43 (22) (2004) 2955–2958.
- [43] A.C. Ferrari, J. Robertson, *Phys. Rev. B: Condens. Matter* 61 (20) (2000) 14095–14107.
- [44] A.S. Amarasekara, L.D. Williams, C.C. Ebede, *Carbohydr. Res.* 343 (18) (2008) 3021–3024.
- [45] S. Caratzoulas, D.G. Vlachos, *Carbohydr. Res.* 346 (5) (2011) 664–672.
- [46] Y. Yang, Z. Du, J. Ma, F. Lu, J. Zhang, J. Xu, *ChemSusChem* 7 (5) (2014) 1352–1356.
- [47] A.A. Rosatella, S.P. Simeonov, R.F.M. Frade, C.A.M. Afonso, *Green Chem.* 13 (4) (2011) 754–793.
- [48] H. Zhu, Q. Cao, C. Li, X. Mu, *Carbohydr. Res.* 346 (13) (2011) 2016–2018.
- [49] J. Wang, W. Xu, J. Ren, X. Liu, G. Lu, Y. Wang, *Green Chem.* 13 (10) (2011) 2678–2681.
- [50] L.J. Konwar, J. Boro, D. Deka, *Renewable Sustainable Energy Rev.* 29 (0) (2014) 546–564.
- [51] S.H. Mushrif, S. Caratzoulas, D.G. Vlachos, *Phys. Chem. Chem. Phys.* 14 (8) (2012) 2637–2644.